Controllable and large-scale supramolecular vesicle aggregation: Orthogonal light-responsive host-guest and metal-ligand interactions†

Guangyan Du[a,b] Lingyun Lou,[b] Shuwen Guan,[b] Yuanyuan Peng,[b]
Hongwei Qiao,[c] Pingli Liu[d] and Dan Wu,[a,*]

[a]*College of Materials Science and Engineering, Zhejiang University of Technology, Hangzhou City 310014, P. R. China.*
[b]*College of Chemistry and Chemical Engineering, Southwest Petroleum University, Chengdu City 610500, P. R. China.*
[c]*Shangdong Tengxi New Materials Co., Ltd, Taian City 271000, P. R. China.*
[d]*State Key Laboratory of Oil and Gas Reservoir Geology and Exploitation, Southwest Petroleum University, Chengdu City 610500, P. R. China.*
E-mail address: danwu@zjut.edu.cn

Electronic Supplementary Information (22 pages)

*1. Synthesis of compound **5***

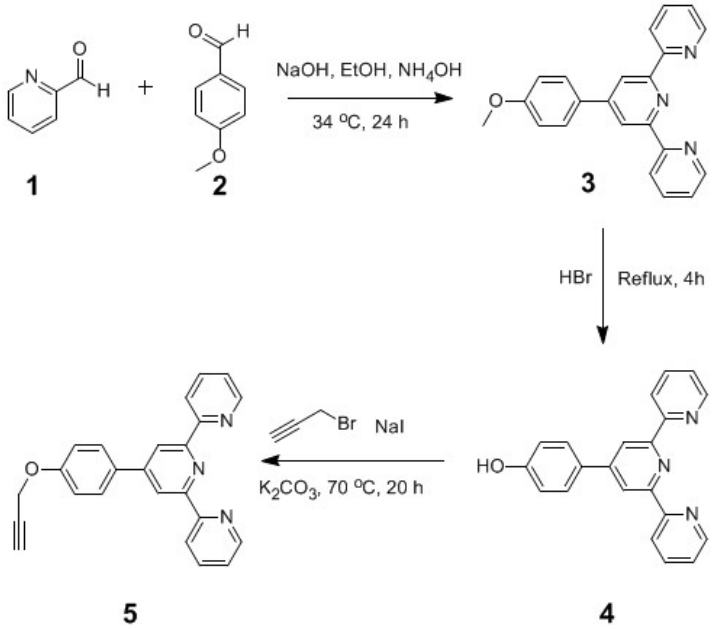

Scheme S1. Synthetic route to **5**.

The ^{1}H NMR spectrum of **3** is shown in Fig. S1. ^{1}H NMR (400 MHz, $CDCl_3$, room temperature) δ (ppm): 8.77−8.69 (m, 4H), 8.67 (d, 2H), 7.88 (t, 4H), 7.40−7.31 (m, 2H), 7.03 (d, 2H), 3.89 (s, 3H). The ^{13}C NMR spectrum of **3** is shown in Fig. S2. ^{13}C NMR (125 MHz, $CDCl_3$, room temperature) δ (ppm): 160.53, 156.40, 155.84, 149.78, 149.10, 136.85, 130.77, 128.54, 123.75, 121.37, 118.30, 114.33, 55.39. HRMS (ESI) m/z calc. for $C_{22}H_{17}N_3O$, $[M+H]^+$ 340.1444; found: 340.1438. The IR spectrum of **3** is shown in Fig. S3.

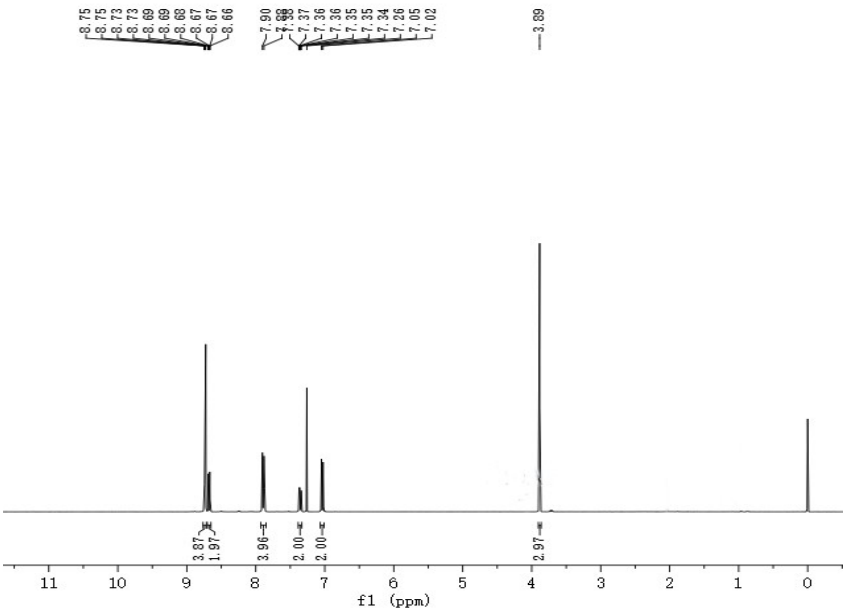

Fig. S1 ^{1}H NMR spectrum (400 MHz, $CDCl_3$, room temperature) of **3**.

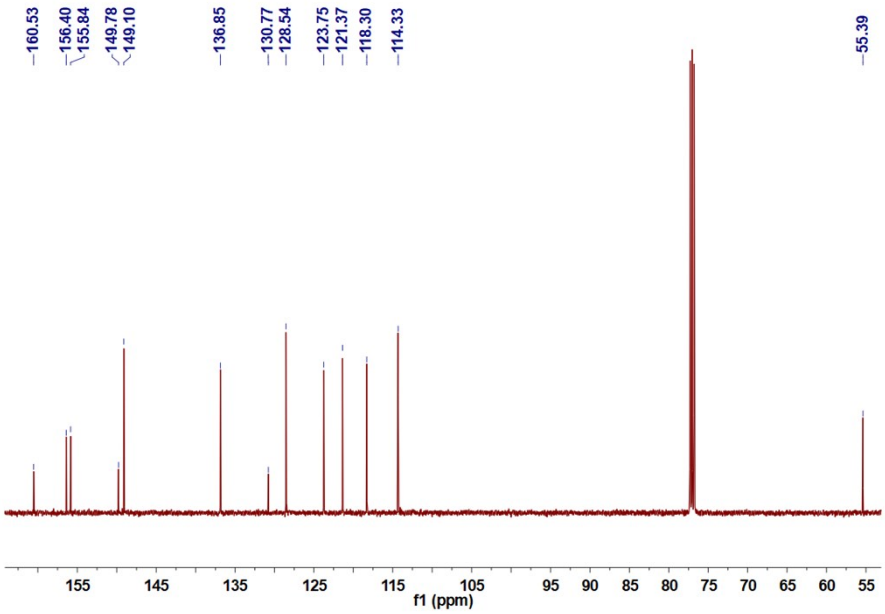

Fig. S2 ^{13}C NMR spectrum (125 MHz, $CDCl_3$, room temperature) of **3**.

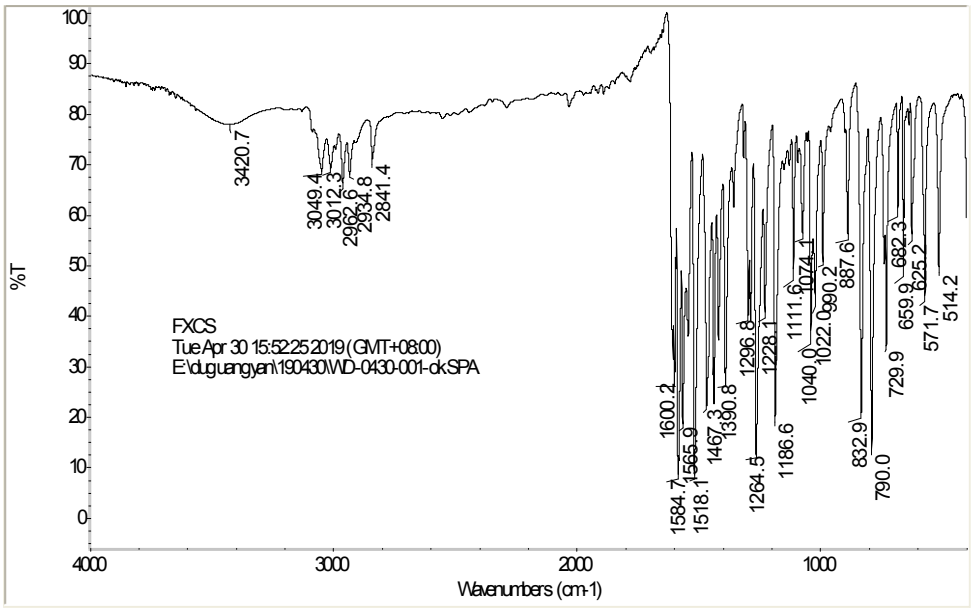

Fig. S3 IR spectrum of **3**.

The ^{1}H NMR spectrum of **4** is shown in Fig. S4. ^{1}H NMR (500 MHz, DMSO-d_6, room temperature) δ (ppm): 9.93 (s, 1H), 8.75 (d, 2H), 8.66−8.64 (m, 4H), 8.03−8.00 (m, 2H), 7.79−7.77 (d, 2H), 7.52−7.50 (m, 2H), 6.98−6.96 (d, 2H). The ^{13}C NMR spectrum of **4** is shown in Fig. S5. ^{13}C NMR (125 MHz, DMSO-d_6, room temperature) δ (ppm): 158.97, 155.49, 155.13, 149.28, 137.39, 128.19, 127.88, 124.38, 120.86, 117.02,

116.21. HRMS (ESI) m/z calc. for $C_{21}H_{15}N_3O$, $[M+H]^+$ 326.1288; found: 326.1280. The IR spectrum of **4** is shown in Fig. S6.

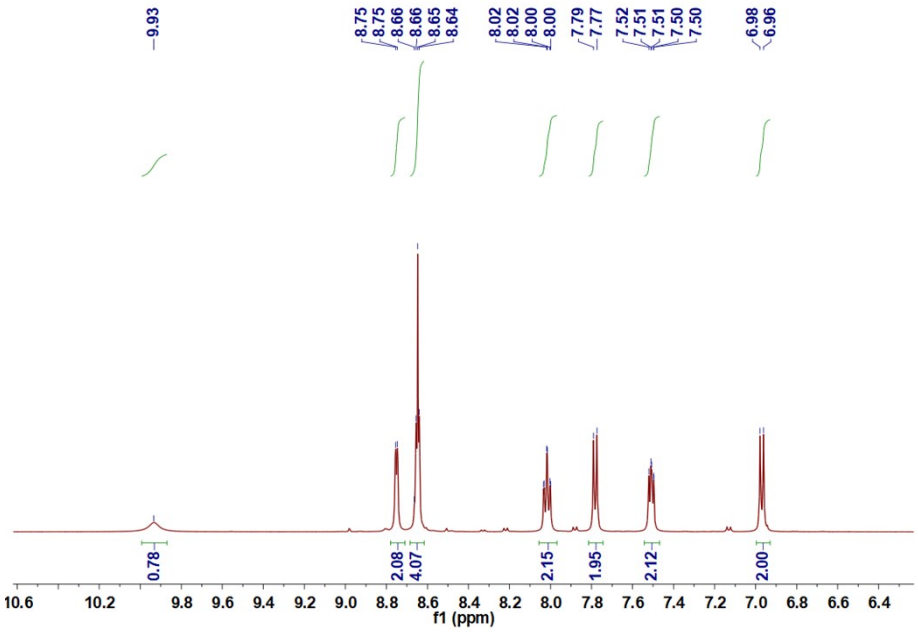

Fig. S4 ^{1}H NMR spectrum (500 MHz, DMSO-d_6, room temperature) of **4**.

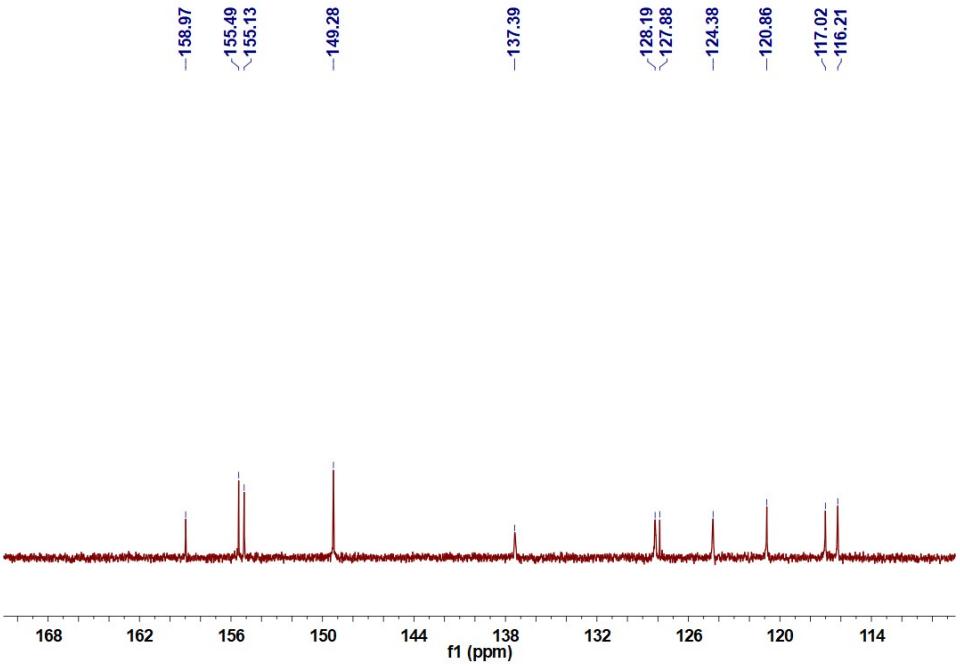

Fig. S5 ^{13}C NMR spectrum (125 MHz, DMSO-d_6, room temperature) of **4**.

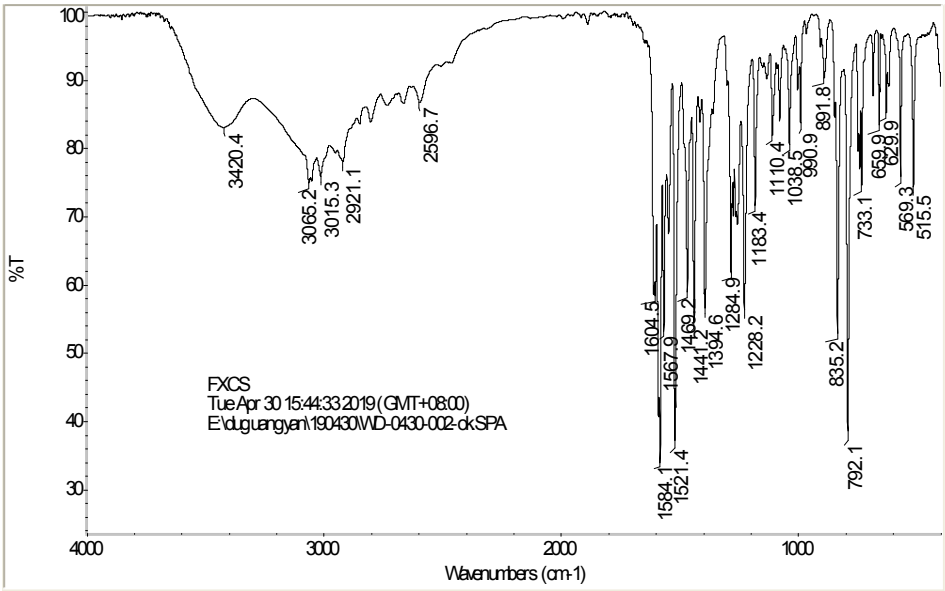

Fig. S6 IR spectrum of **4**.

The ^{1}H NMR spectrum of **5** is shown in Fig. S7. ^{1}H NMR (500 MHz, $CDCl_3$, room temperature) δ (ppm): 8.74−8.72 (m, 4H), 8.69−8.67 (d, 2H), 7.91−7.87 (m, 4H), 7.37−7.35 (m, 2H), 7.13−7.11 (m, 2H), 2.59−2.58 (t, 1H). The ^{13}C NMR spectrum of **5** is shown in Fig. S8. ^{13}C NMR (125 MHz, $CDCl_3$, room temperature) δ (ppm): 136.86, 131.74, 128.57, 123.78, 121.36, 118.31, 115.30, 114.33, 78.32, 75.80, 55.90. HRMS (ESI) m/z calc. for $C_{24}H_{17}N_3O$ $[M+H]^+$ 364.1444; found: 364.1437. The IR spectrum of **5** is shown in Fig. S9.

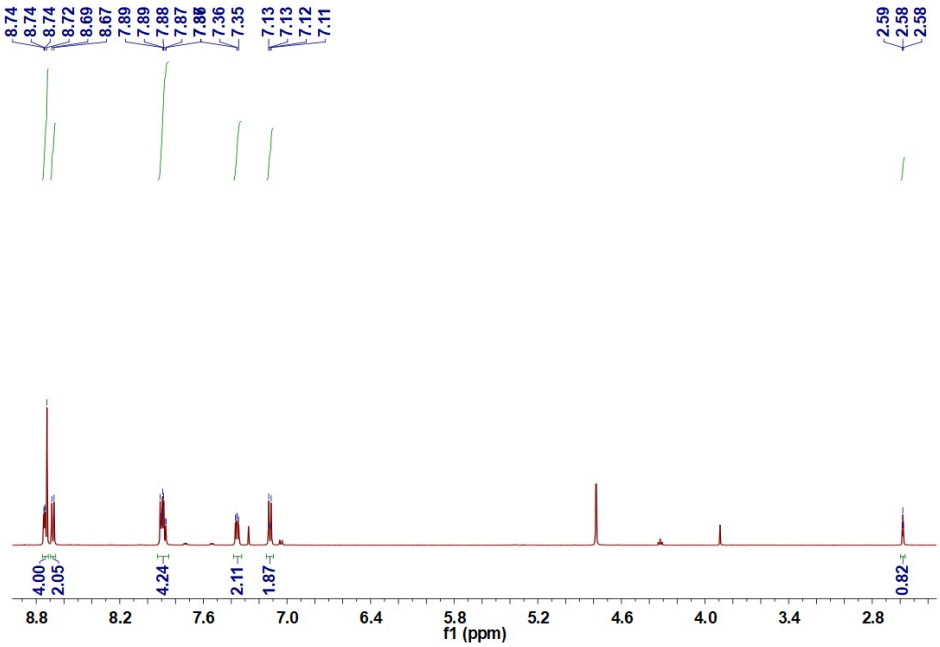

Fig. S7 ^{1}H NMR spectrum (500 MHz, $CDCl_3$, room temperature) of **5**.

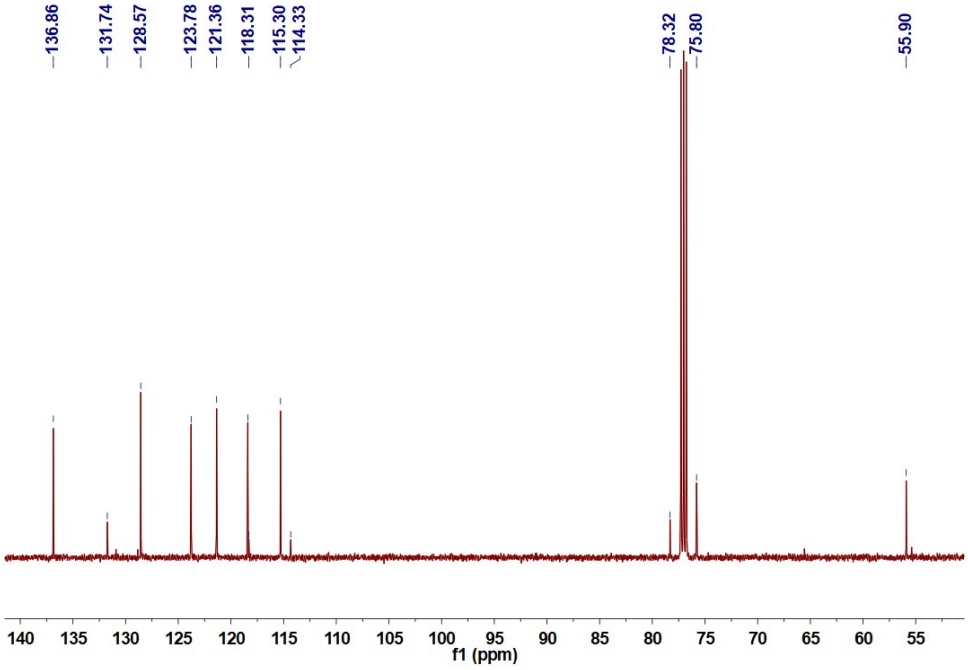

Fig. S8 ^{13}C NMR spectrum (125 MHz, $CDCl_3$, room temperature) of **5**.

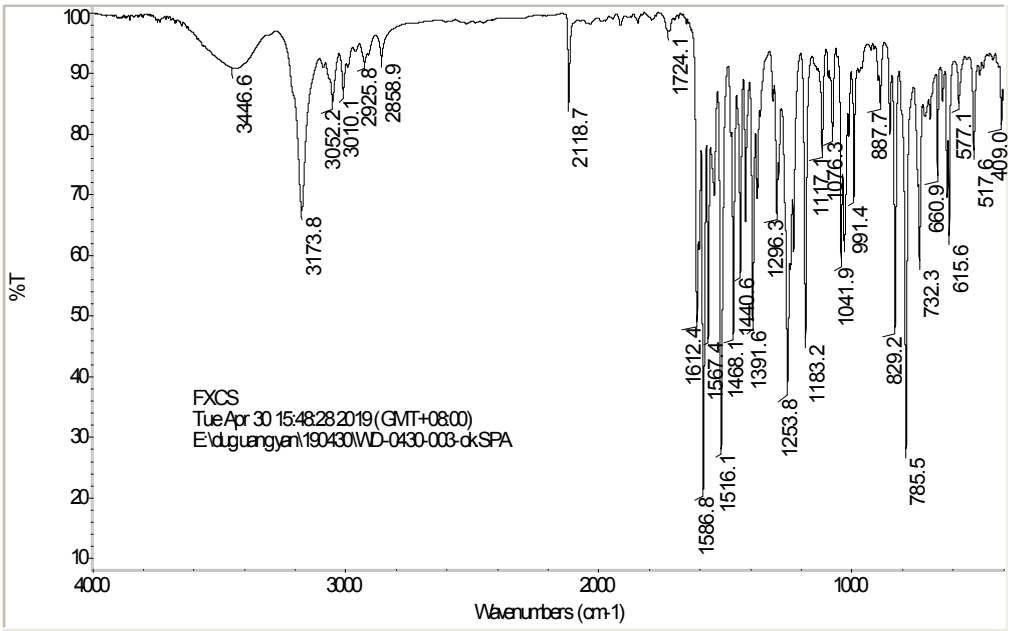

Fig. S9 IR spectrum of **5**.

2. The synthesis of compound ***Py-CD***

Scheme S2. Synthetic route to **Py-CD**.[S1-S2]

The ^{1}H NMR spectrum of **7** is shown in Fig. S10. ^{1}H NMR (500 MHz, DMSO-d_6, room temperature) δ (ppm): 7.76−7.70 (m, 2H), 7.48−7.40 (m, 2H), 4.84−4.83 (m, 5H), 4.77−4.76 (m, 2H), 4.33−4.31 (m, 1H), 4.20−4.17 (m, 2H), 3.71−3.19 (m, 41H), 2.43−2.41 (d, 3H). HRMS (ESI) m/z calc. for $C_{49}H_{76}O_{37}S$ $[M+H]^+$ 1311.3678; found: 1311.3638. The IR spectrum of **7** is shown in Fig. S11.

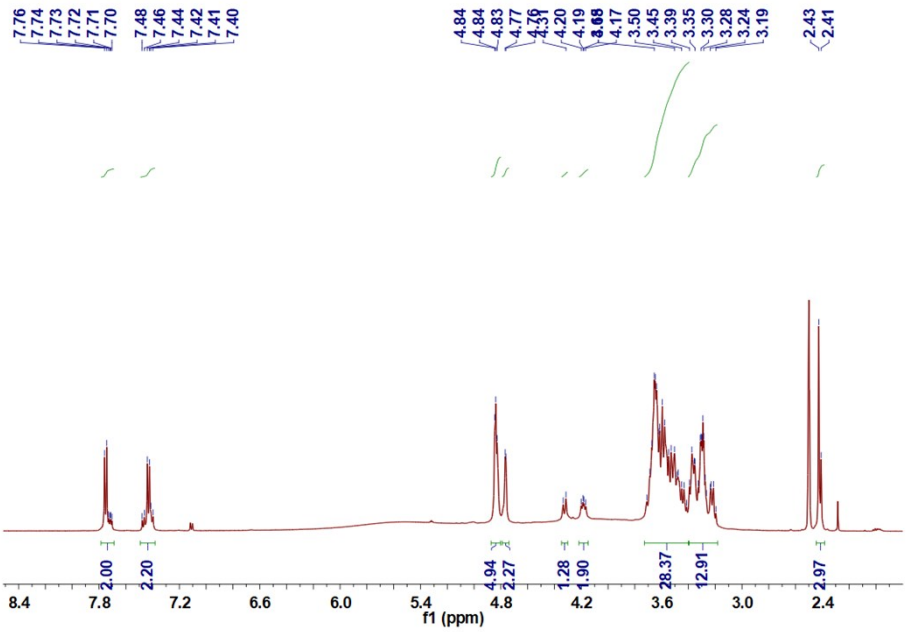

Fig. S10 ^{1}H NMR spectrum (500 MHz, DMSO-d_6, room temperature) of **7**.

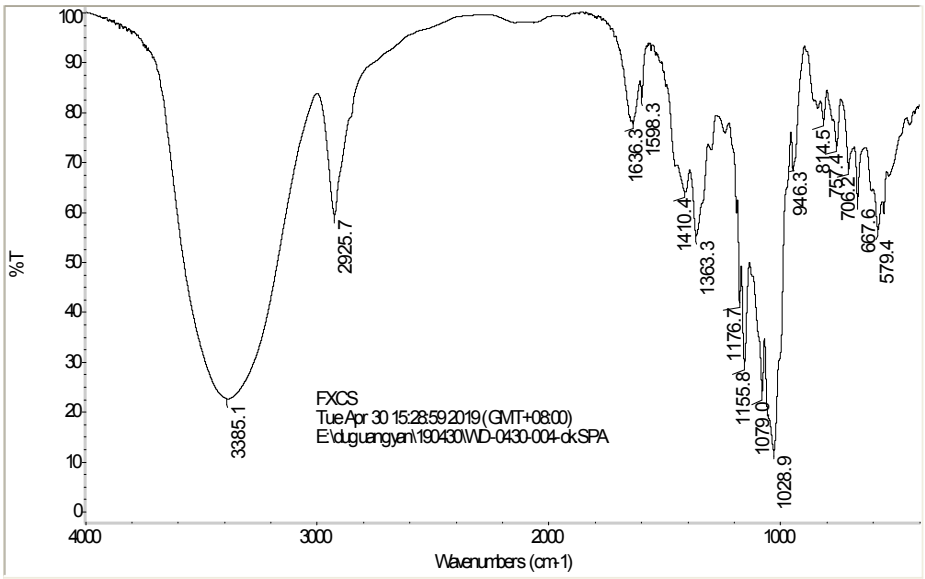

Fig. S11 IR spectrum of **7**.

The ^{1}H NMR spectrum of **8** is shown in Fig. S12. ^{1}H NMR (400 MHz, $CDCl_3$, room temperature) δ (ppm): 5.72 (s, 14H), 4.88−4.82 (m, 7H), 4.46 (s, 6H), 3.78−3.56 (m, 31H). HRMS (ESI) m/z calc. for $C_{42}H_{69}N_3O_{34}Na$ $[M+Na]^+$ 1182.3655; found: 1182.3633. The IR spectrum of **8** is shown in Fig. S13.

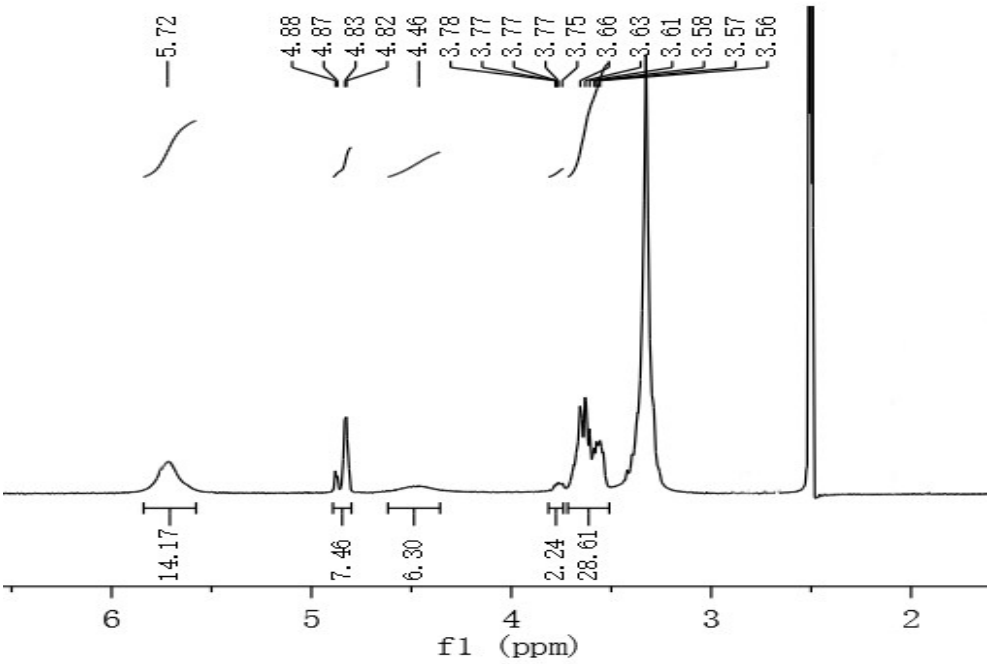

Fig. S12 ^{1}H NMR spectrum (400 MHz, $CDCl_3$, room temperature) of **8**.

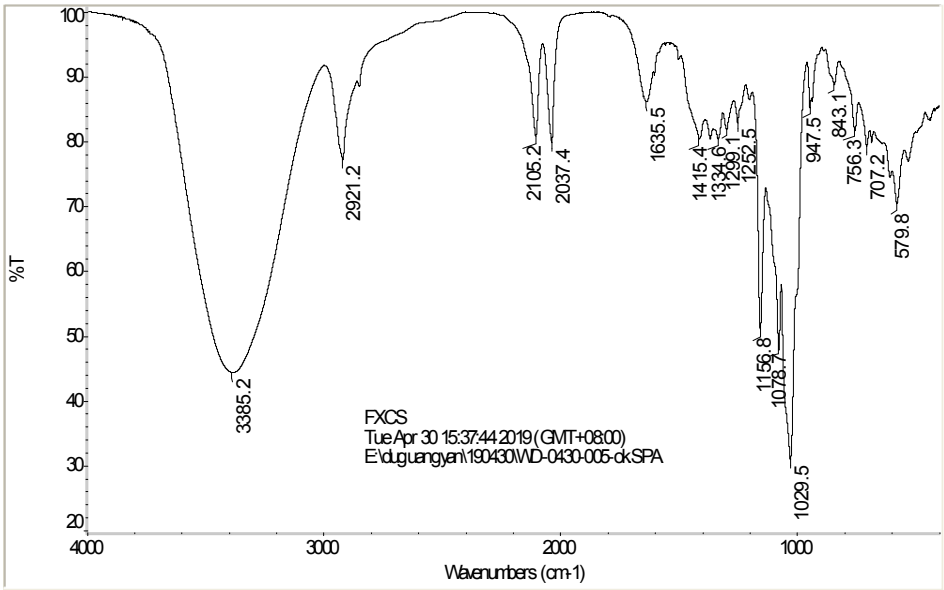

Fig. S13 IR spectrum of **8**.

The ^{1}H NMR spectrum of **Py-CD** is shown in Fig. S14. ^{1}H NMR (400 MHz, DMSO-d_6, room temperature) δ (ppm): 8.78 (d, 2H), 8.70 (d, 4H), 8.23 (s, 1H), 8.06 (t, 2H), 7.93 (d, 2H), 7.59–7.52 (m, 2H), 7.27 (d, 2H), 5.72 (s, 14H), 5.21 (s, 2H), 5.05 (d, 2H), 4.90–4.76 (m, 7H), 4.69–4.56 (m, 3H), 3.65 (ddd, 29H), 3.54–3.07 (m, 64H). HRMS (ESI) m/z calc. for $C_{66}H_{86}N_6O_{35}$ 1523.5207; found: m/z $[M+H]^+$ 1523.5142. The IR spectrum of **Py-CD** is shown in Fig. S15.

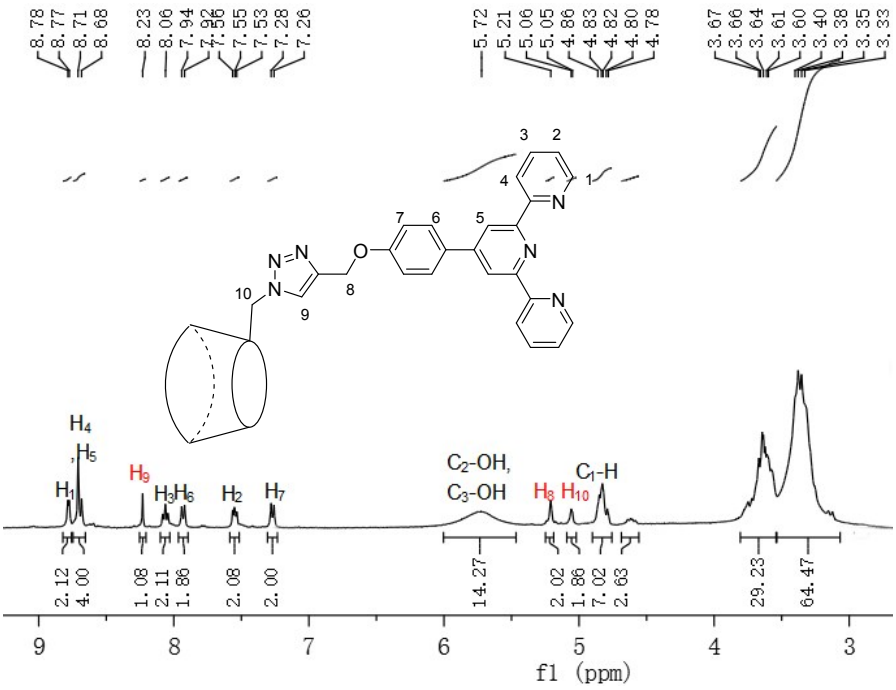

Fig. S14 ^{1}H NMR spectrum (400 MHz, DMSO-d_6, room temperature) of **Py-CD**.

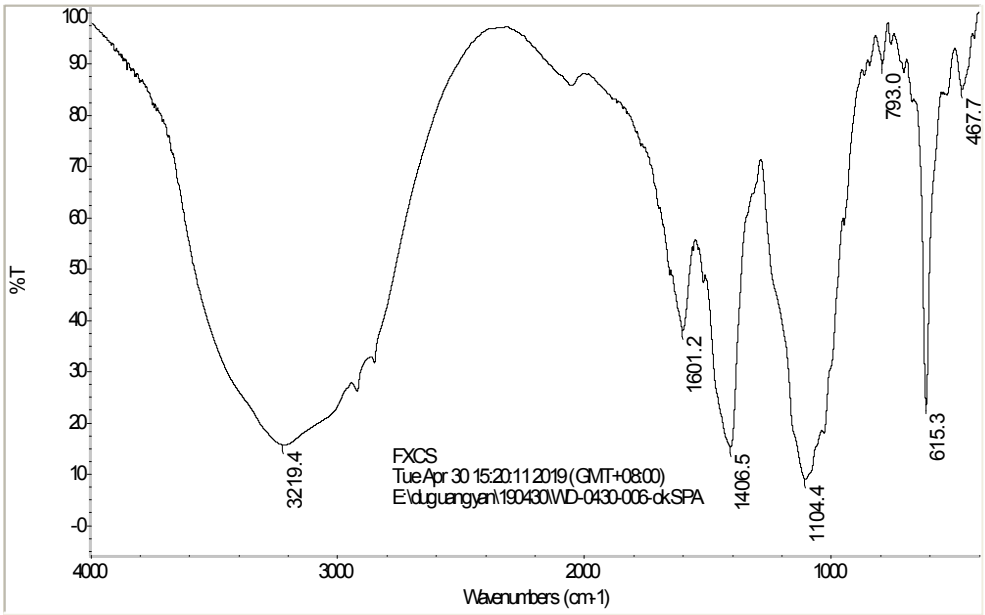

Fig. S15 IR spectrum of **Py-CD**.

*3. Synthesis of compounds **Azo-C** and **Azo-C$_3$***

Scheme S3. Synthetic route of **Azo-C** *and* **Azo-C$_3$**.[S3-S6]

The ^{1}H NMR spectrum of **Azo-C** is shown in Fig. S16. ^{1}H NMR (400 MHz, $CDCl_3$, room temperature) δ (ppm): 7.92–7.87 (m, 4H), 7.53–7.47 (m, 2H), 7.44 (d, 1H), 7.00 (d, 2H), 4.04 (t, 2H), 1.86–1.78 (m, 2H), 1.27 (s, 16H), 0.91–0.86 (m, 3H). HRMS (ESI)

m/z calc. for $C_{24}H_{34}N_2O$ $[M+H]^+$ 367.2744; found: 367.2732. The IR spectrum of **Azo-C** is shown in Fig. S17.

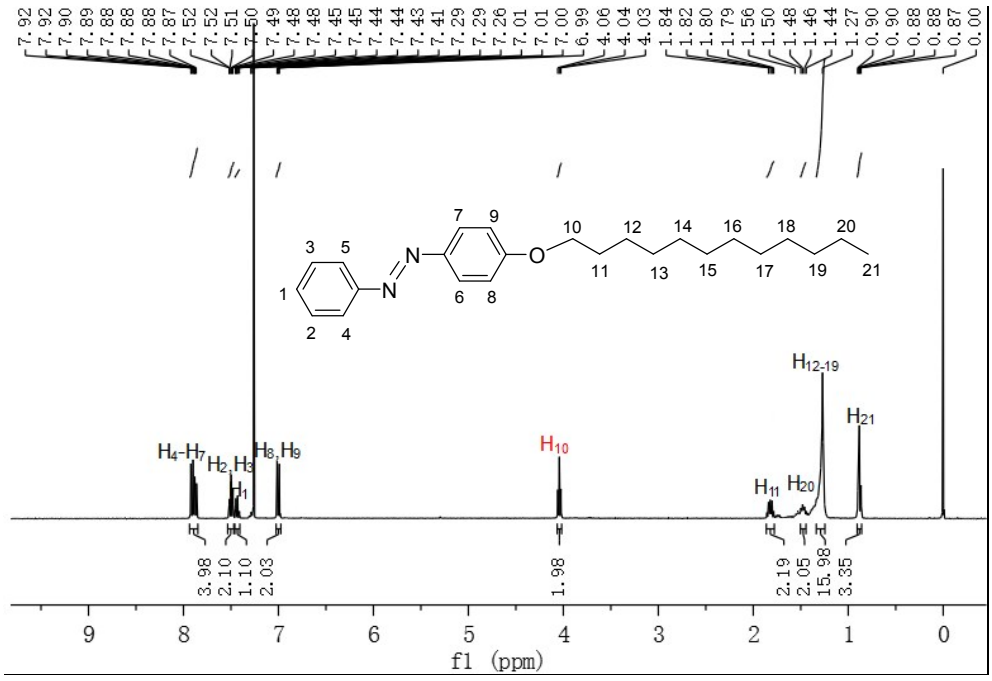

Fig. S16 ^{1}H NMR spectrum (400 MHz, $CDCl_3$, room temperature) of **Azo-C**.

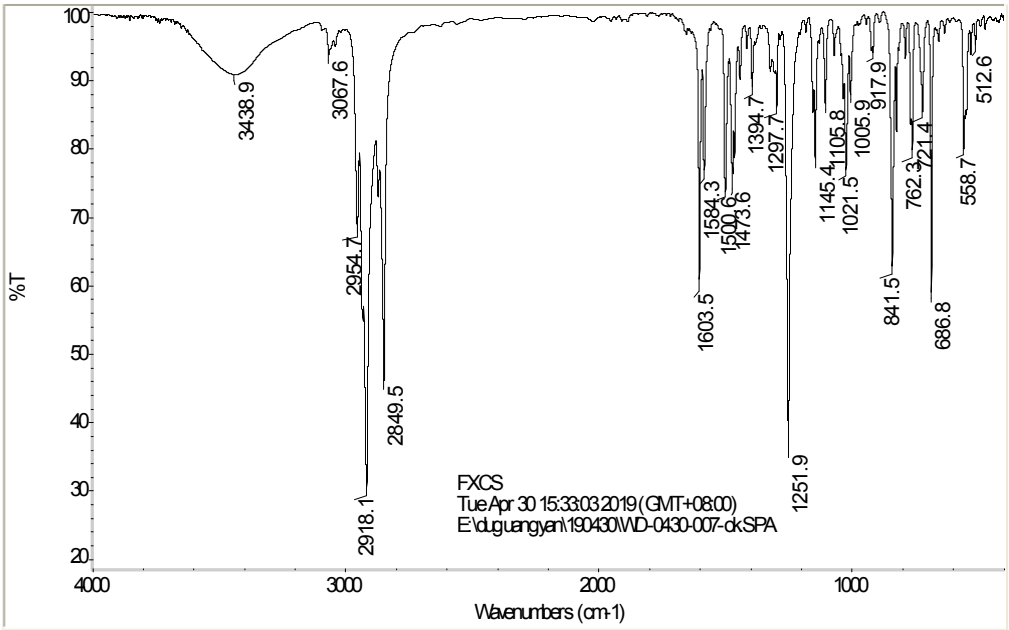

Fig. S17 IR spectrum of **Azo-C**.

The ^{1}H NMR spectrum of **12** is shown in Fig. S18. ^{1}H NMR (400 MHz, $CDCl_3$, room temperature) δ 7.25 (d, 2H), 4.01 (m, 6H), 3.89 (s, 3H), 1.83–1.71 (m, 6H), 1.33–1.24 (m, 48H), 0.88 (t, 9H). The ^{13}C NMR spectrum of **12** is shown in Fig. S19. ^{13}C NMR

(125 MHz, $CDCl_3$, room temperature) δ (ppm): 166.97, 161.21, 152.85, 142.42, 124.67, 108.03, 73.51, 69.20, 64.15, 52.10, 29.68, 29.59, 29.51, 29.39, 29.33, 28.53, 26.08, 22.71, 14.12. HRMS (ESI) m/z calc. for $C_{44}H_{80}O_5$ $[M+Na]^+$ 711.5898; found: 711.5883. The IR spectrum of **12** is shown in Fig. S20.

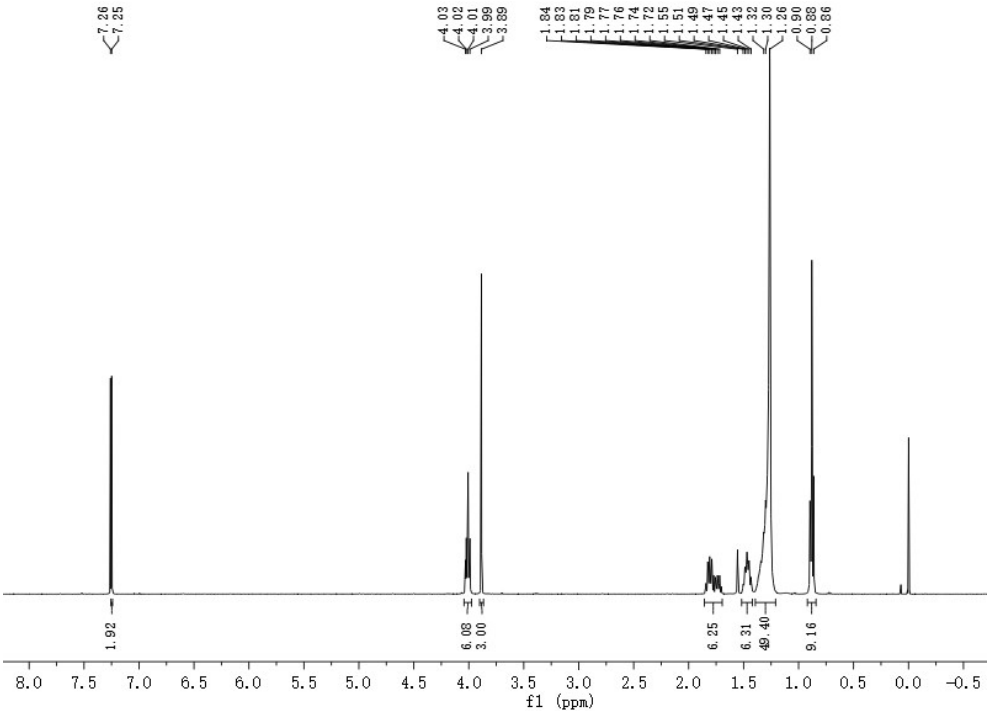

Fig. S18 ^{1}H NMR spectrum (400 MHz, $CDCl_3$, room temperature) of **12**.

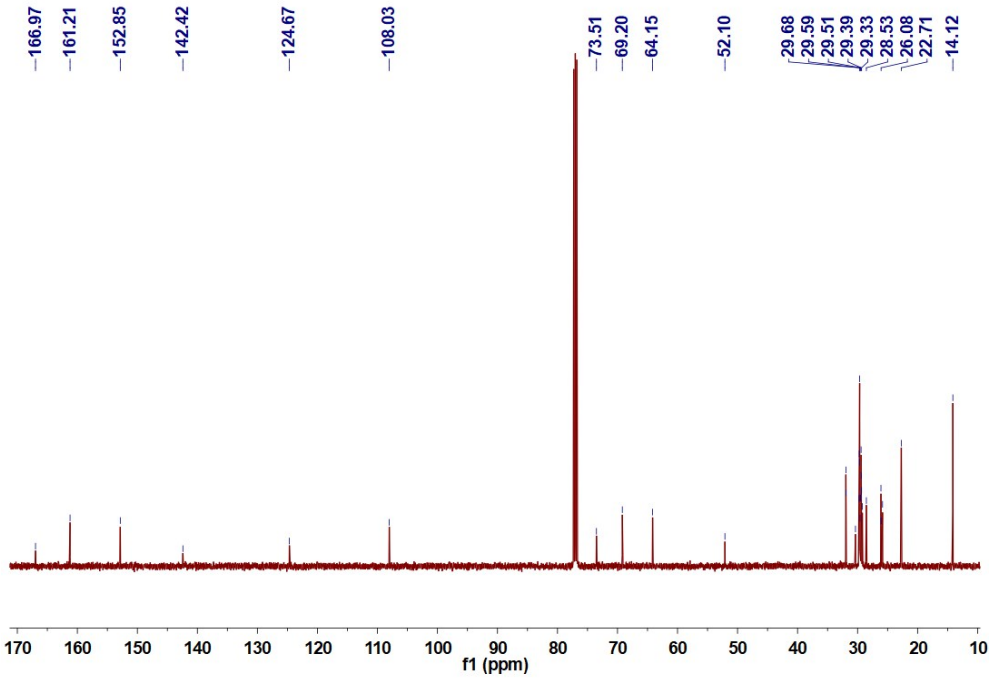

Fig. S19 ^{13}C NMR spectrum (125 MHz, $CDCl_3$, room temperature) of **12**.

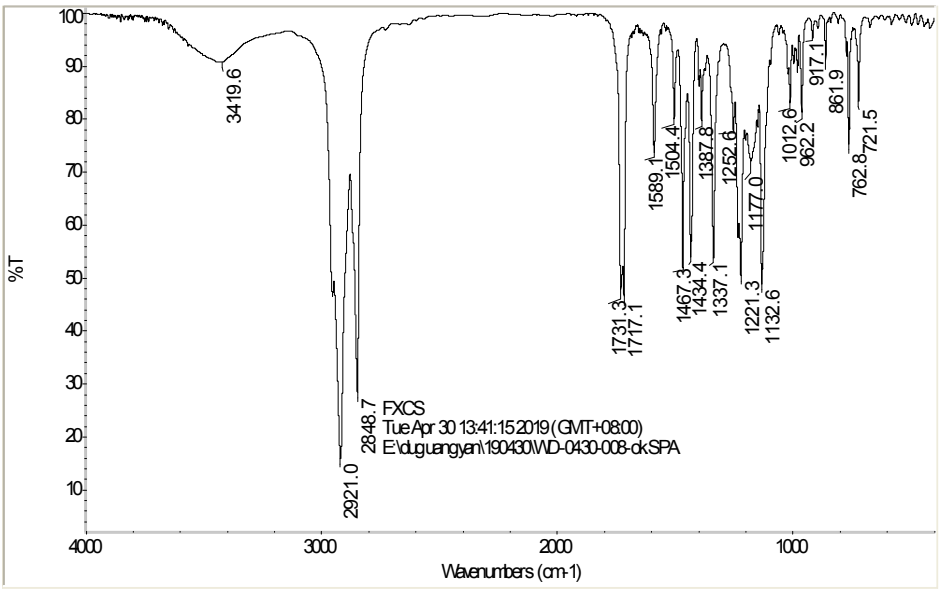

Fig. S20 IR spectrum of **12**.

The ^{1}H NMR spectrum of **13** is shown in Fig. S21. ^{1}H NMR (400 MHz, $CDCl_3$, room temperature) δ 7.31 (s, 2H), 4.06–4.00 (m, 6H), 1.85–1.72 (m, 6H), 1.34–1.25 (m, 49H), 0.90–0.86 (m, 9H). The ^{13}C NMR spectrum of **13** is shown in Fig. S22. ^{13}C NMR (125 MHz, $CDCl_3$, room temperature) δ (ppm): 171.48, 152.88, 143.20, 123.62, 108.61, 77.28, 77.03, 76.78, 73.58, 69.23, 63.15, 29.72, 29.66, 29.59, 29.42, 29.39, 29.31, 26.10, 26.07, 22.72, 14.13. HRMS (ESI) m/z calc. for $C_{43}H_{78}O_5$ $[M+H]^+$ 697.5741; found: 697.5730. The IR spectrum of **13** is shown in Fig. S23.

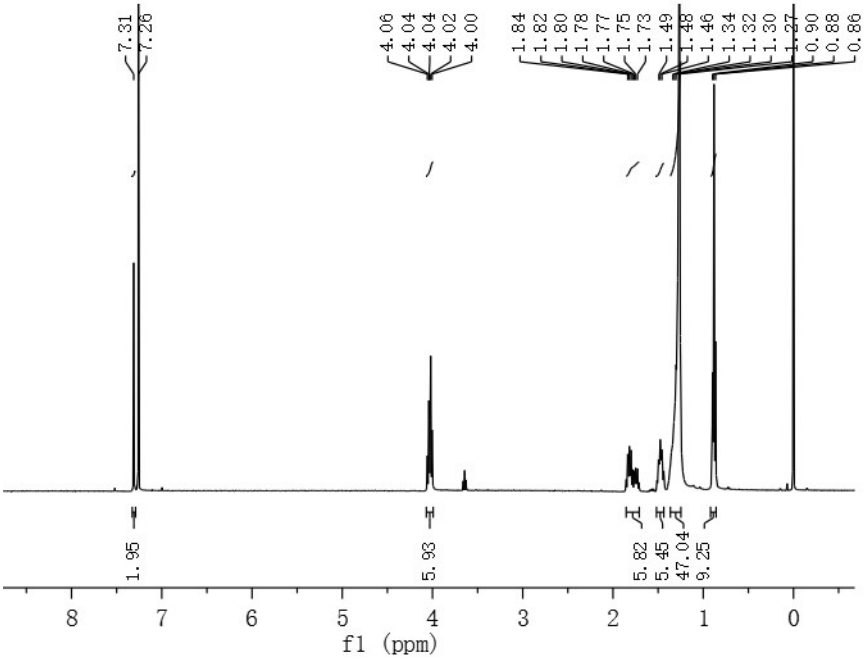

Fig. S21 ^{1}H NMR spectrum (400 MHz, $CDCl_3$, room temperature) of **13**.

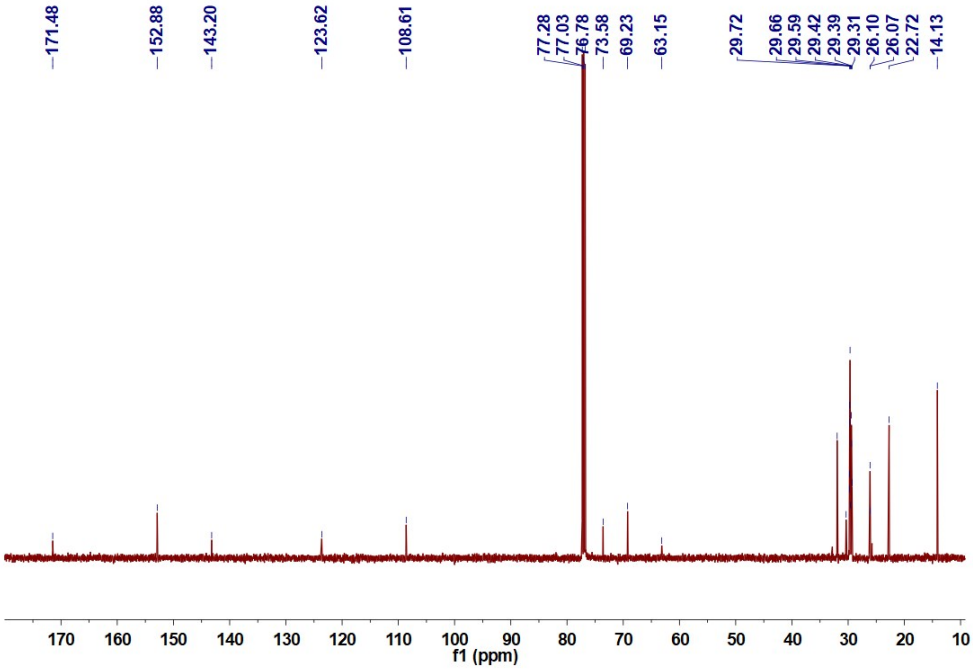

Fig. S22 ^{13}C NMR spectrum (125 MHz, $CDCl_3$, room temperature) of **13**.

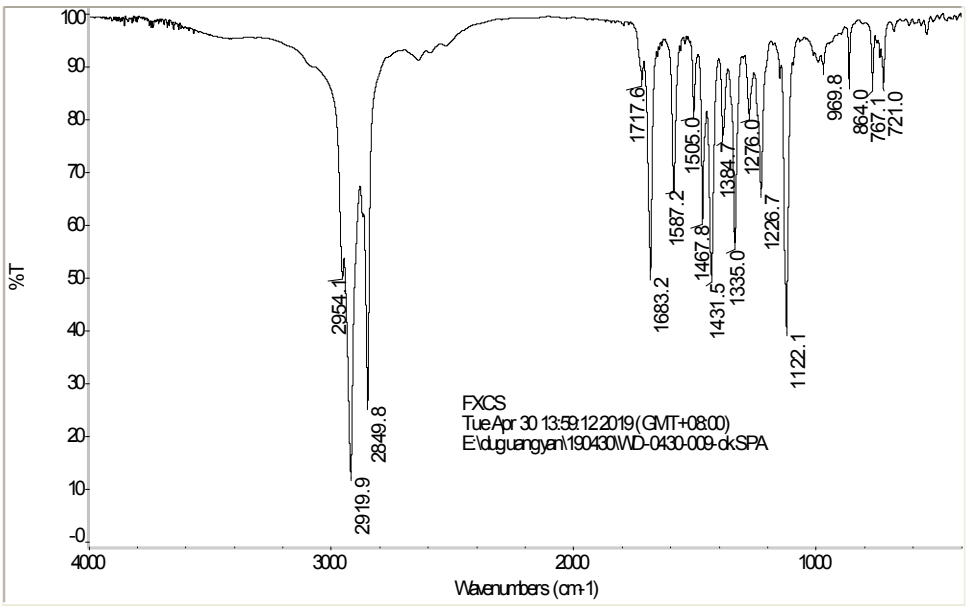

Fig. S23 IR spectrum of **13**.

The ^{1}H NMR spectrum of **Azo-C$_3$** is shown in Fig. S24. ^{1}H NMR (400 MHz, $CDCl_3$, room temperature) δ 7.99–7.96 (m, 2H), 7.92 (dd, 2H), 7.84–7.79 (m, 2H), 7.54–7.44 (m, 3H), 7.07 (s, 2H), 4.03 (q, 6H), 1.80 (m, 6H), 1.5–1.45 (m, 6H), 1.34–1.24 (m, 48H), 0.90–0.86 (m, 9H). The IR spectrum of **Azo-C$_3$** is shown in Fig. S26.

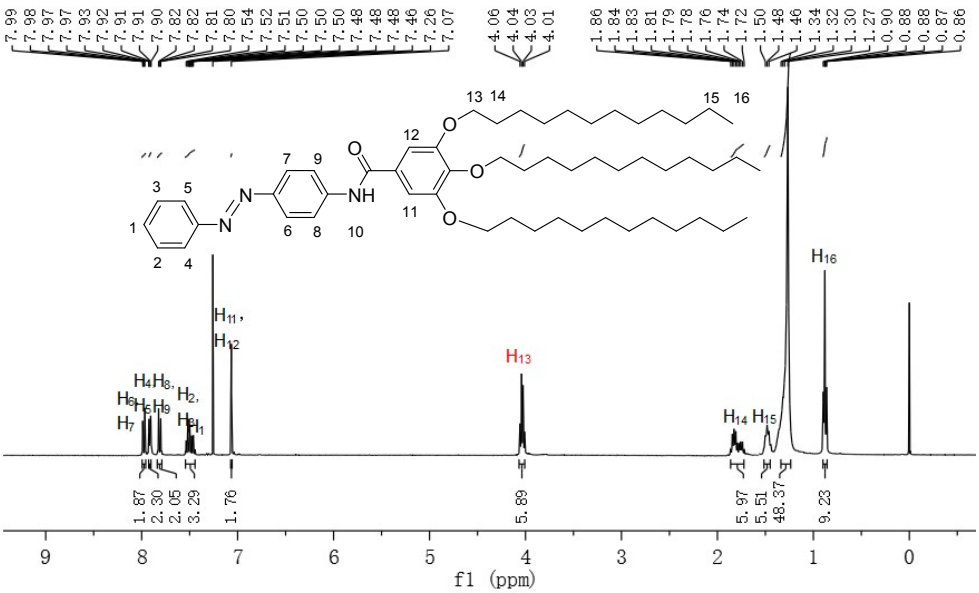

Fig. S24 ^{1}H NMR spectrum (400 MHz, $CDCl_3$, room temperature) of **Azo-C$_3$**.

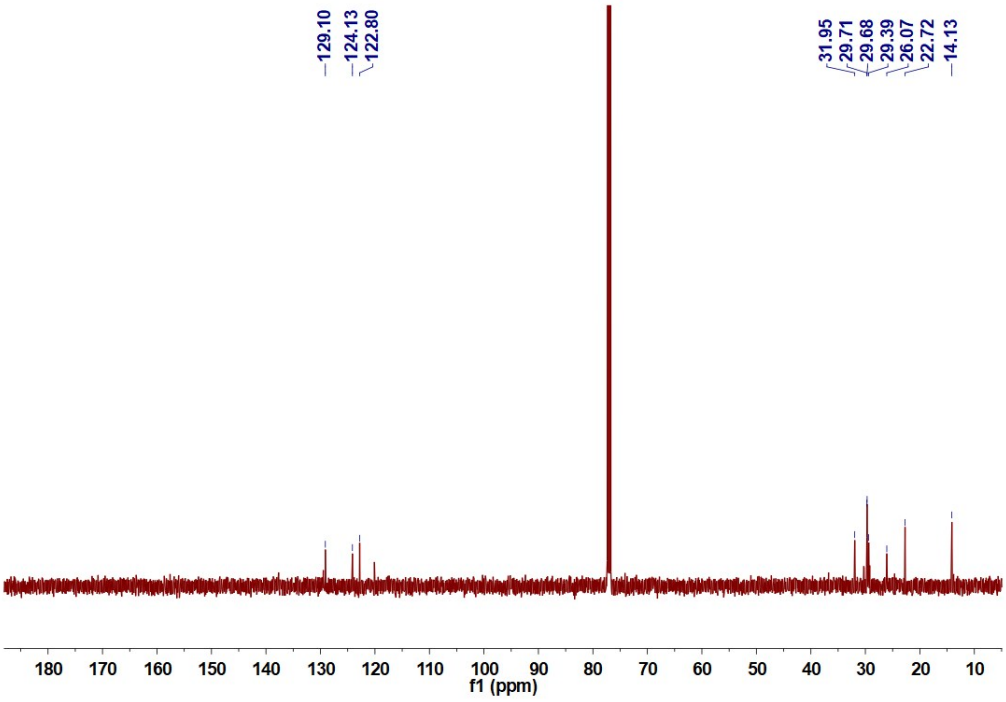

Fig. S25 ^{13}C NMR spectrum (125 MHz, $CDCl_3$, room temperature) of **Azo-C$_3$**.

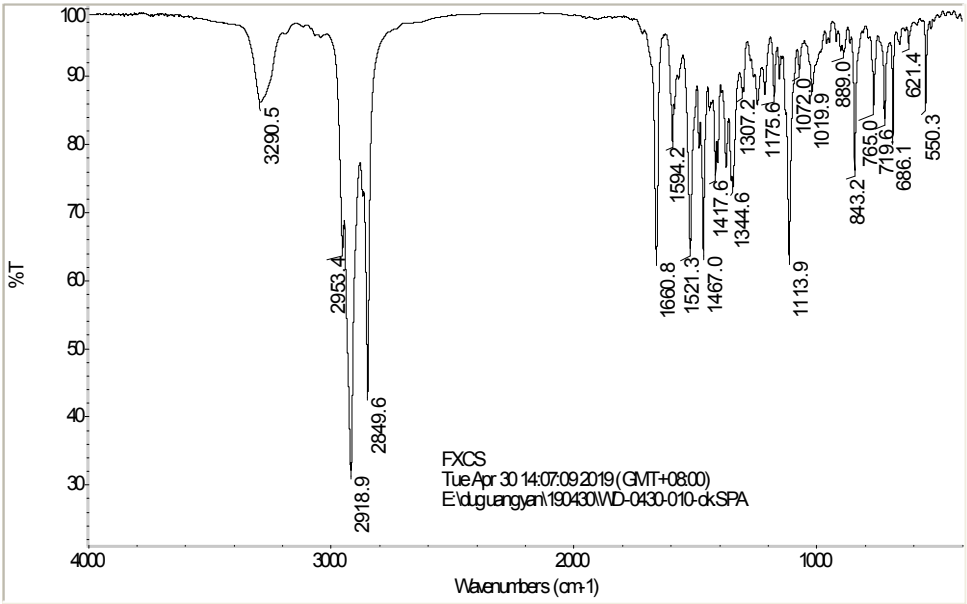

Fig. S26 IR spectrum of **Azo-C$_3$**.

*4. Particle size distributions of **Azo-C** and **Azo-C$_3$**.*

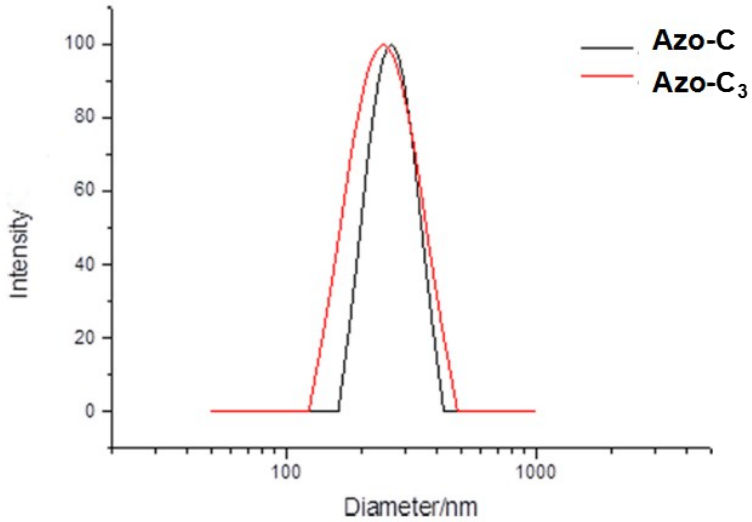

Fig. S27 Particle size distributions of **Azo-C** and **Azo-C$_3$**.

*5. The Tyndall effect in the series of **Azo-C** and **Azo-C$_3$** THF/H$_2$O solutions.*

Fig. S28 The Tyndall effect in the series of **Azo-C** (upper) and **Azo-C$_3$** (below) THF/H_2O solutions.

*6. Investigations of trans–cis photoisomerization of **Py-CD⊃Azo-C** and **Py-CD⊃Azo-C$_3$** under different irradiation conditions.*

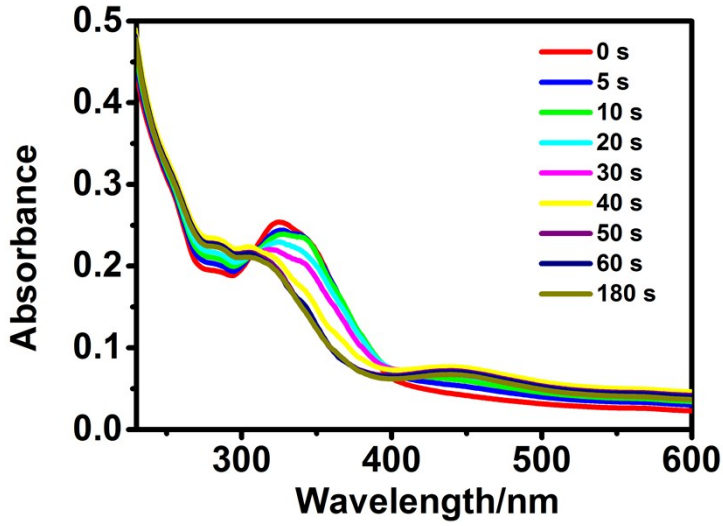

Fig. S29 UV spectra of **Py-CD⊃Azo-C** under UV light irradiation at different time points (UV light = 365 nm).

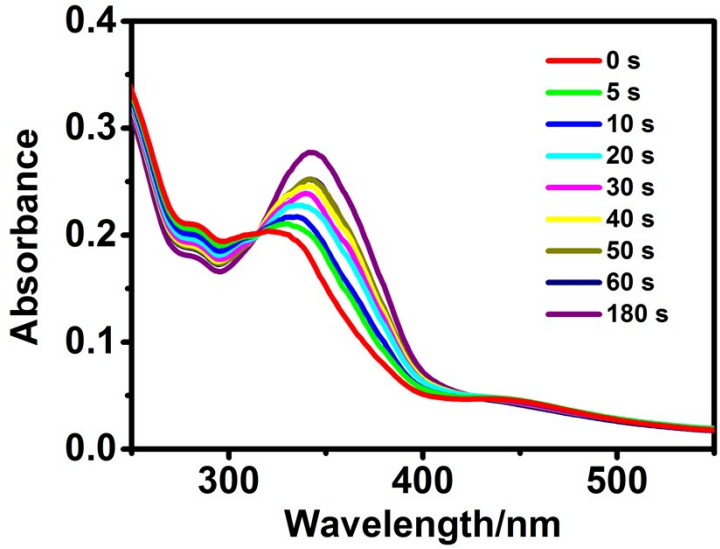

Fig. S30 UV spectra of **Py-CD⊃Azo-C** which had been irradiated by UV light under visible light irradiation at different time points (UV light = 365 nm, visible light = 450 nm).

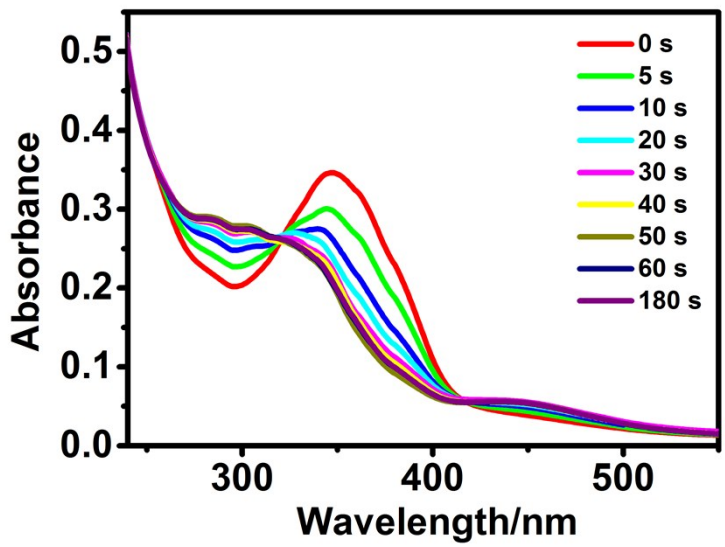

Fig. S31 UV spectra of **Py-CD⊃Azo-C$_3$** under UV light irradiation at different time points (UV light = 365 nm).

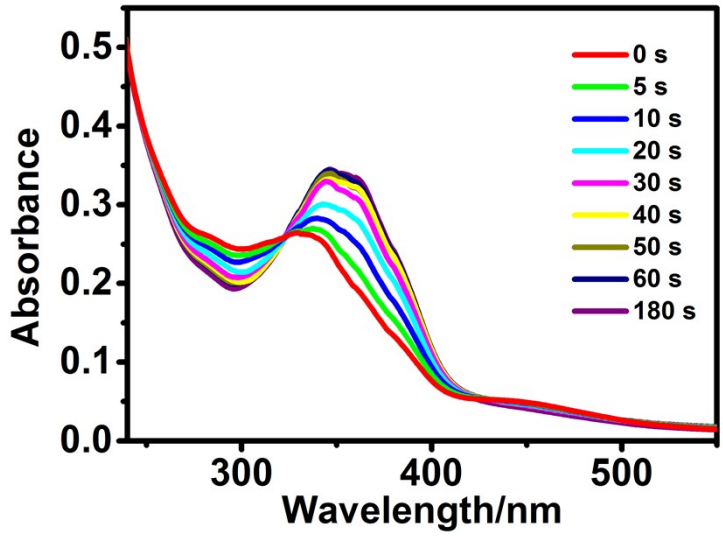

Fig. S32 UV spectra of **Py-CD⊃Azo-C$_3$** which had been irradiated by UV light under visible light irradiation at different time points (UV light = 365 nm, visible light = 450 nm).

*7. Partial ^{1}H NMR spectra of **Py-CD**, **Azo-C**, **Azo-C$_3$**, **Py-CD⊃Azo-C** and **Py-CD⊃Azo-C$_3$**.*

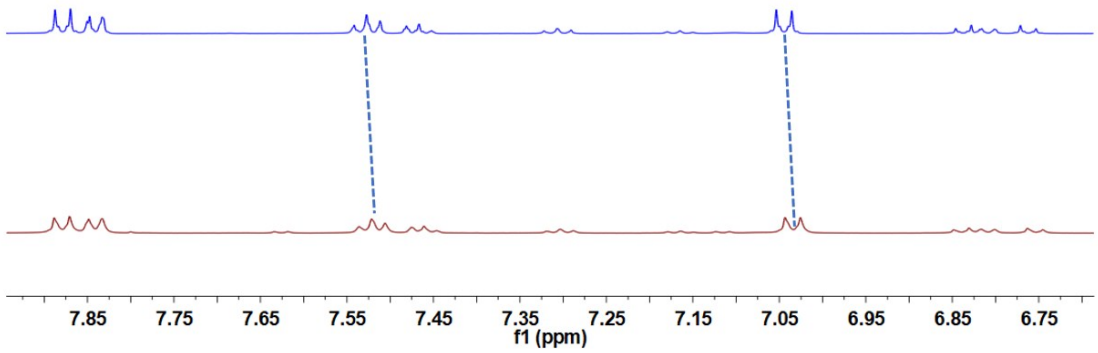

Fig. S33 Partial ^{1}H NMR spectra ($CHCl_3$/DMSO-d_6, room temperature, 500 MHz) of **Azo-C** (blue) and **Py-CD⊃Azo-C** (red).

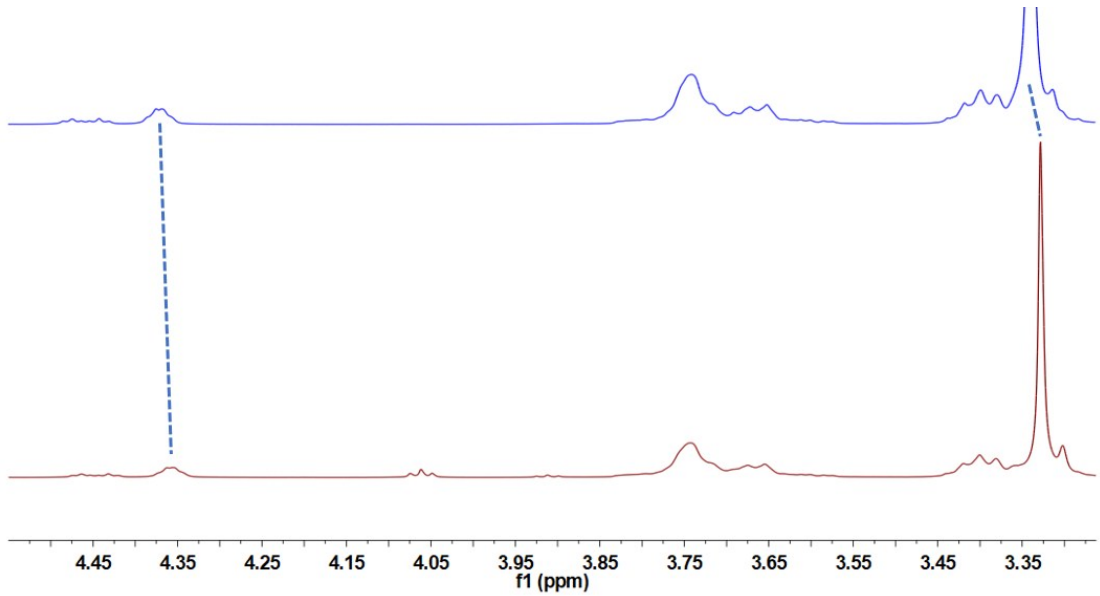

Fig. S34 Partial ^{1}H NMR spectra ($CHCl_3$/DMSO-d_6, room temperature, 500 MHz) of **Py-CD** (blue) and **Py-CD⊃Azo-C** (red).

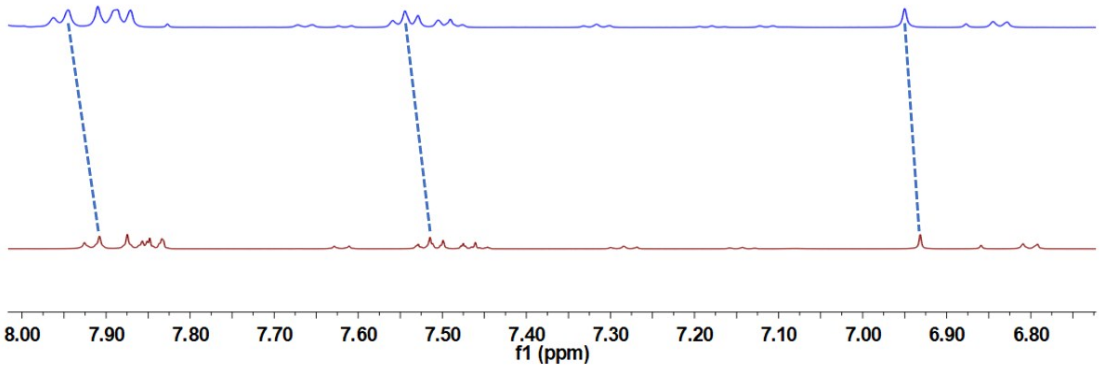

Fig. S35 Partial ^{1}H NMR spectra ($CHCl_3$/DMSO-d_6, room temperature, 500 MHz) of **Azo-C$_3$** (red) and **Py-CD⊃Azo-C$_3$** (blue).

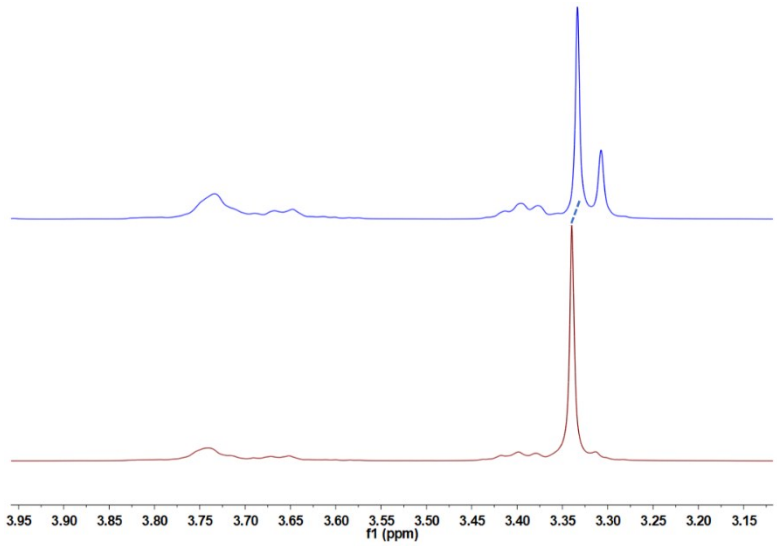

Fig. S36 Partial ^{1}H NMR spectra ($CHCl_3$/DMSO-d_6, room temperature, 500 MHz) of **Py-CD** (red) and **Py-CD⊃Azo-C$_3$** (blue).

*8. The color change of **Azo-C** and **Azo-C$_3$** solutions before and after complexation.*

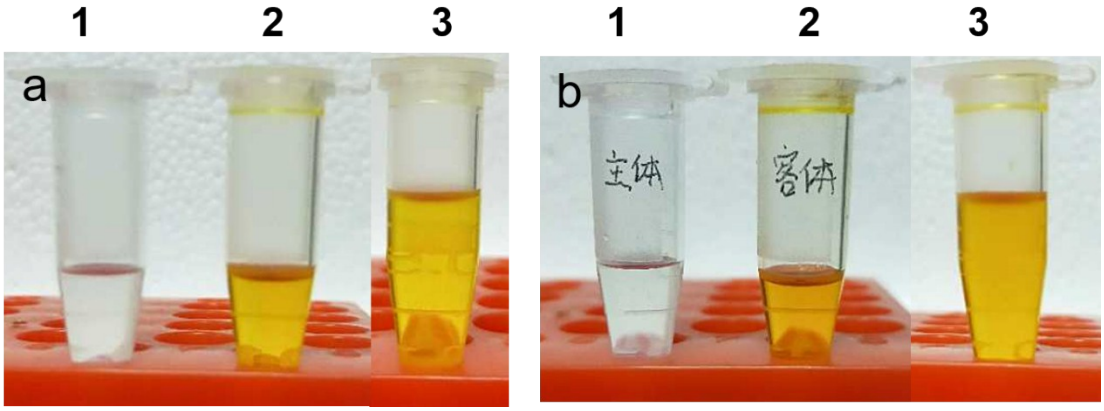

Fig. S37 Color change of **Azo-C** (a) and **Azo-C$_3$** (b) solution before and after complexation (1: **Py-CD**; 2: **Azo-C**; 3: **Py-CD⊃Azo-C** or **Py-CD⊃Azo-C$_3$**).

*9. Cytotoxicity evaluation and internalization behavior of **Py-CD⊃Azo-C** and **Py-CD⊃Azo-C$_3$**.*

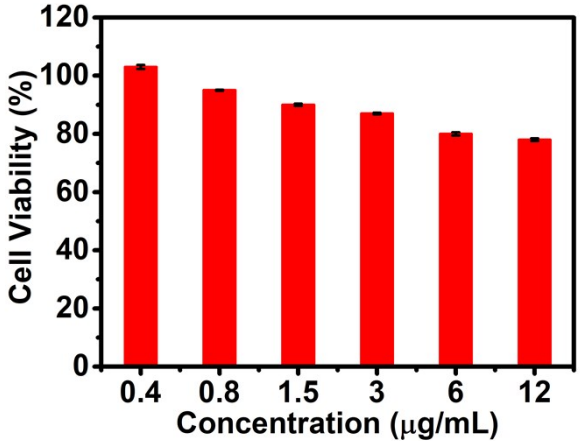

Fig. S38 Cytotoxicity of 293T cells by culturing with the **Py-CD⊃Azo-C** with different concentrations for 24 h.

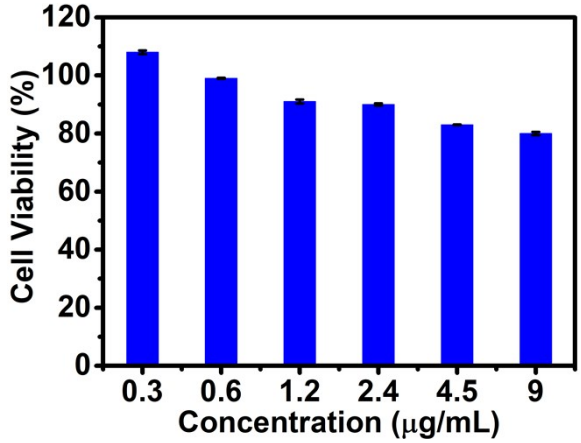

Fig. S39 Cytotoxicity of 293T cells by culturing with the **Py-CD⊃Azo-C$_3$** with different

concentrations for 24 h.

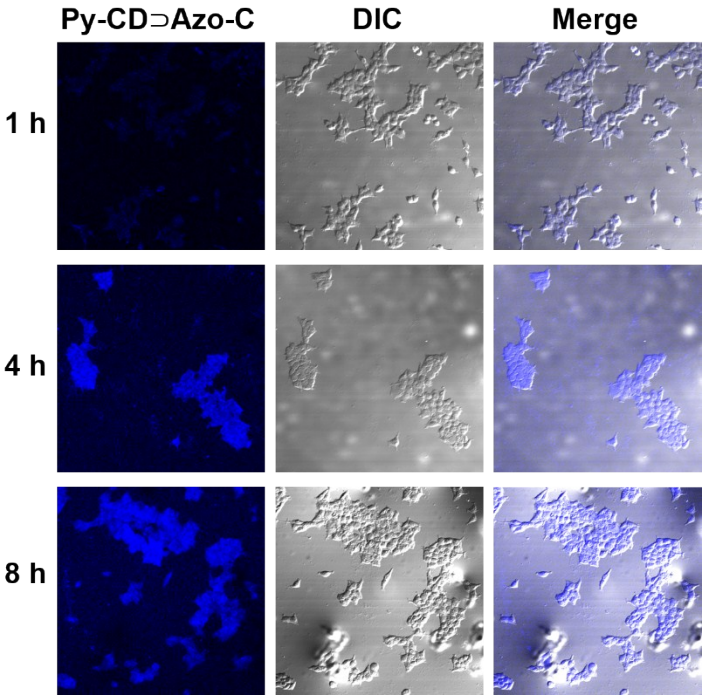

Fig. S40 Confocal images of 293T cells incubated with **Py-CD⊃Azo-C** for different time periods.

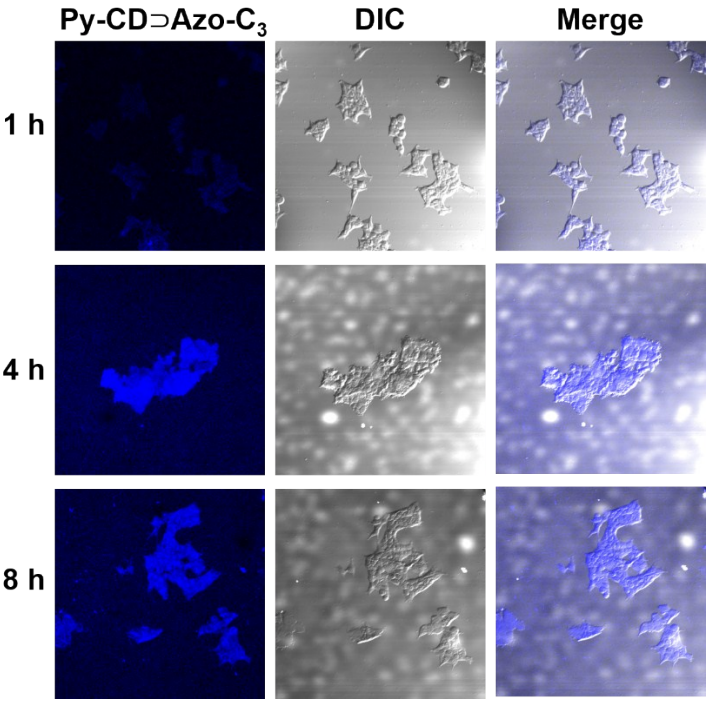

Fig. S41 Confocal images of 293T cells incubated with **Py-CD⊃Azo-C_3** for different time periods.

References:

S1. B. Brady, N. Lynam, T. O'Sullivan, C. Ahern and R. Darcy, *Org. Synth.*, 2000, **77**, 220−224.

S2. C. Hocquelet, J. Blu, C. K. Jankowski, S. Arseneau, D. Buisson and L. Mauclaire, *Tetrahedron*, 2006, **62**, 11963−11971.

S3. Y. M. Chabre, C. Contino-Pépin, V. Placide, T. C. Shiao and R. Roy, *J. Org. Chem.*, 2008, **73**, 5602−5605.

S4. M. D. Tzirakis, M. N. Alberti, H. Weissman, B. Rybtchinski and F. Diederich, *Chem. Eur. J.*, 2014, **20**, 16070−16073.

S5. S. Zhang, H.-J. Sun, A. D. Hughes, B. Draghici, J. Lejnieks, P. Leowanawat, A. Bertin, L. O. D. Leon, O. V. Kulikov, Y. Chen, D. J. Pochan, P. A. Heiney and V. Percec, *ACS Nano*., 2014, **8**, 1554−1565.

S6. J. Zou, F. Tao and M. Jiang, *Langmuir*, 2007, **23**, 12791−12794.